Monthly Notices of the ROYAL ASTRONOMICAL SOCIETY
MNRAS **525,** 1936–1940 (2023) https://doi.org/10.1093/mnras/stad2428
Advance Access publication 2023 August 17

Line-of-sight optical Dome Turbulence Monitor

James Osborn [1]★ and David Alaluf[2]
[1]*Centre for Advanced Instrumentation, Department of Physics, Durham University, DH1 3LE, Durham, UK*
[2]*European Space Agency - ESA/ESTEC, Keplerlaan 1, NL-2200 AG Noordwijk, the Netherlands*

Accepted 2023 August 2. Received 2023 July 13; in original form 2023 April 26

ABSTRACT

Optical turbulence in the enclosure of a ground-based telescope can be a major contributor to the total optical turbulence strength and can therefore limit the precision of astronomical observations, in terms of angular resolution, or signal to noise ratio, depending on the instrumentation used. Here we propose a new Dome Turbulence Monitor (DTM) technique. This DTM is based on the well known Scintillation Detection And Ranging (SCIDAR) concept with a few major differences. By designing the instrument specifically for the dome turbulence, we can use a small (<0.2 m telescope), and observe single bright stars (as opposed to the SCIDAR using double stars). This enables a dedicated instrument with enough targets to operate continuously. Operationally, the DTM could be mounted somewhere on the main astronomical telescope and track stars that are visible through the dome aperture. By measuring through the dome aperture we obtain an optical measure of the strength of the turbulence along a similar line of sight as the main telescope itself. We demonstrate the new technique through numerical Monte Carlo modelling and present results from a proof-of-concept demonstration at the European Space Agency Optical Ground Station on Tenerife, Spain.

Key words: atmospheric effects – instrumentation: Adaptive Optics – site testing.

1 INTRODUCTION

Optical turbulence in the Earth’s atmosphere limits the performance of ground-based telescopes. Local turbulence within and around a telescope structure, often called dome turbulence, can be a significant contribution to the total turbulence strength.

Among the causes of dome turbulence, one can for instance quote: equipment releasing heat inside the dome (e.g. Cassegrain instruments, motors, computers, lasers), lights, persons, thermal history, and properties of components creating surface-air temperature gradients, air flows entering the dome creating local eddies etc. This local turbulence can be minimized by reducing any temperature differences along the optical path. This can include actively cooling any surfaces, such as mirrors, and thermalizing the dome such that the internal and external temperatures match. The latter can take the form of opening the dome or any hatches/louvre and using fans to deliberately mix the air. Care must be taken, however, when actively controlling the temperature of a component (e.g. mirror) to avoid it to behave as a moisture trap which could damage it (Woolf 1979). Multifaceted shapes of domes can also be considered so as to ‘break’ dome eddies stemming from air flows entering through the slit of the dome. In any case, without a method to measure the turbulence in the dome, it is difficult to optimize this strategy.

In addition, when designing optical instruments and Adaptive Optics systems, great care is taken to understand the strength and distribution of the atmospheric optical turbulence, but very little is known about the turbulence generated and confined in or around the dome. A quantitative measurement would enable a more precise measure of the local turbulence and therefore a better model of expected instrument performance.

Point spread function (PSF) reconstruction techniques can be used to estimate the optical PSF (Beltramo-Martin et al. 2020). Augmenting these models with measured dome turbulence contributions could lead to improved performance.

Observing programs can be selected based on estimated Image Quality (IQ). This IQ depends on the integrated turbulence in the atmosphere but also the turbulence in the dome. Without sufficient dome turbulence monitoring the latter is unknown and could contribute a significant fraction of the total turbulence. A complexity here is that the IQ depends on the nature of the turbulence as well as the strength (Tokovinin 2002).

As Bustos & Tokovinin (2018) point out, all turbulence monitoring instrumentation involve imposing a model to extract quantitative measurements from the raw data. These models assume stationary statistics, which is not necessarily the case with confined turbulence. Therefore, it is important to note, with all of these techniques that although a quantitative measurement of the confined optical turbulence strength can be estimated, linking this to the delivered IQ of a large telescope is inherently uncertain. It is possible to make assumptions which would enable a quantitative IQ estimation, such as assuming dome turbulence to be von Kármán turbulence with an outer scale of a few metres, but this remains to be validated.

The measurements can however be used as a relative quantitative estimate in order to minimize the magnitude of the turbulence. In addition, the scintillation based method proposed here is insensitive to the power spectrum of the phase. Although this could be seen as a limitation on the information available, it is advantageous in that

★ E-mail: james.osborn@durham.ac.uk

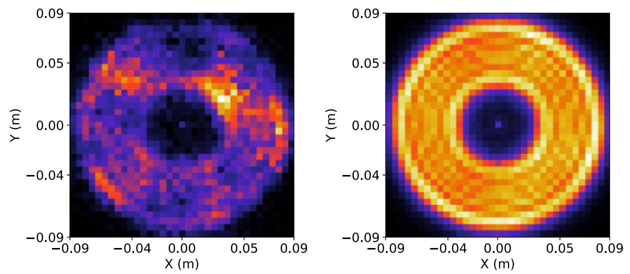

Figure 1. Simulated conjugate pupil images at +450 m. Left is instantaneous image and right is average image.

the data analysis does not need to take this into account, which can be complicated for phase-based methods.

There are very few studies that do attempt to estimate the quantitative effect on the IQ of the large telescope. A study by Racine et al. (1991) for the Canada France Hawaii Telescope does this statistically by making the assumption that dome turbulence is correlated with the internal – external temperature difference. They then examine the full width at half-maximum of the image on one of their instruments against this temperature difference. It is found that the median dome turbulence contribution is approximately 0.1 arcsec. However, as expected, this increases with increasing temperature difference, reaching 0.4 arcsec at an internal – external temperature difference of 3.5 degrees Centigrade.

Combining dome turbulence measurements with external site monitoring instrumentation would enable better reactive queue scheduling for observatories.

Some techniques for measuring the optical turbulence within the dome already exist. Most methods involve laser beam propagation across the turbulence medium.

For example, the 'Local Turbulence Experiment' (Berdja et al. 2013) and its development, the INdoor TurbulENce SEnsor (Chabé et al. 2016), use a number of parallel laser beams to probe the turbulence, across the primary mirror for example. By examining the differential motion as a function of laser beam separation the strength and the phase structure function of the turbulence can be determined.

Bustos & Tokovinin (2018) developed another dome seeing monitor based on a single laser beam propagated from the primary mirror cell to the secondary mirror cell and reflected back. With this instrument the authors measure the delivered IQ, which can be used as a quantitative metric to minimize the turbulence.

Another option is the Airborne Interferometric Recombiner – Fluctuations of Light at Optical Wavelengths (Lai et al. 2019). This instrument again uses a laser beam to probe the turbulent medium but uses a non-redundant pupil mask imaging interferometer, which enables the user to measure the 2D phase structure function, as such it is possible to determine the turbulence strength and the outer scale of the turbulence.

Here, we propose a new confined turbulence measurement device, the Dome Turbulence Monitor (DTM). This instrument is different to the ones outlined above, in that it does not use a laser beam to probe a single path near the telescope. Instead, it uses a star as a light source and view through the enclosure aperture, and therefore, if the instrument is mounted on the primary mirror cell, for example it will have a very similar line of sight as the main telescope. The DTM will target visible bright stars and change target as the main telescope tracks. Obviously it will not include any turbulence due to temperature differentials at the primary mirror surface, but other sources should be visible. This DTM is based on the well known Scintillation Detection And Ranging (SCIDAR) concept (Avila, Vernin & Cuevas 1998; Shepherd et al. 2013) with a few major differences. By designing the instrument specifically for the dome turbulence, we can use a small (<0.2 m telescope), and observe single bright stars (rather than doubles). This enables a dedicated instrument capable of pointing anywhere in the sky.

The DTM concept is presented through numerical simulation and we show the first on-sky demonstration at the European Space Agency (ESA) Optical Ground Station (OGS), Tenerife, Spain.

In Section 2, we describe the method and explore the sensitivity through simulated results, Section 3 shows the on-sky demonstration results from the ESA OGS, Tenerife, Spain, and in Section 4 we present the conclusions.

2 SCINTILLATION BASED DOME TURBULENCE MONITOR

We have developed a turbulence monitoring instrument based on the SCIDAR (Scintillation dome monitoring technique; Avila et al. 1998; Shepherd et al. 2013). However, as we are only interested in the local turbulence only one bright star is required (unlike traditional SCIDAR which uses two stars to estimate the vertical structure of the turbulence).

The concept is to measure a 2D spatial scintillation pattern in a conjugate plane (∼500 m) above the pupil on a small (15 to 20 cm) telescope. The conjugation plane is above the ground (rather than below, cf. SCIDAR) to attenuate the signal from atmospheric turbulent layers.

By mounting the DTM on the side of the main telescope we can estimate the dome turbulence along the line of sight of the experiment. Other dome monitoring system tend to be point measurements or laser based systems probing certain paths, for example across the primary mirror cell. In addition, the scintillation based system is insensitive to the underlying turbulence structure. This is both an advantage and a disadvantage. It means we are less susceptible to model errors, but the turbulence power spectrum could be a useful parameter to know.

Fig. 1 shows a simulated image from an 18 cm telescope with two layer atmosphere with turbulence at 0 m and 10 km above the ground level. The intensity variations are caused by the propagation of the light from the turbulent layers to the detector plane. The simulation is set-up with a high-spatial sampling and down-sampled to the proposed instrument scales in order to avoid biases due to spatial sampling of the simulation. The images show significant diffraction due to the extra propagation distance to the conjugate plane. Shot noise appropriate to a 5th magnitude star in the '*V*'-band is used in order to make the simulation as realistic as possible.

We then calculate spatio-temporal co-variance of the measured intensity pattern (see Fig. 2). At the origin we will measure the scintillation variance of all atmospheric layer signals. However, in the temporal co-variance function, atmospheric layers are separated due to the lateral translation of the turbulence driven by the wind. For the dome turbulence we assume turbulence is constrained in or around the dome and is therefore slowly evolving compared to the atmospheric components which will have wind speeds $>1\,\mathrm{m\,s^{-1}}$. This is the same method used by common SCIDAR systems.

By fitting a temporal decay function to the centre of the spatio-temporal co-variance function and extrapolating to $\mathrm{d}t = 0$, we can extract the dome induced scintillation variance (Fig. 3). Here we use a linear regressive fit to extrapolate the scintillation co-variance to

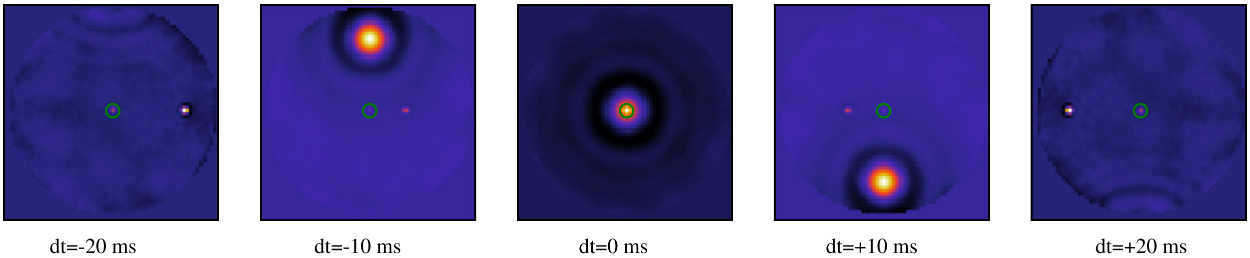

Figure 2. Example spatio-temporal co-variance function from simulation. The green circle indicates the signal due to the dome turbulence, constrained in the centre of the function. The large peak moving top to bottom is the free-atmosphere layer (at 10 km) which moves through the co-variance function with the velocity of the translational wind. The smaller peak moving right to left is the ground layer. Note that the colour scale changes for each image for clarity.

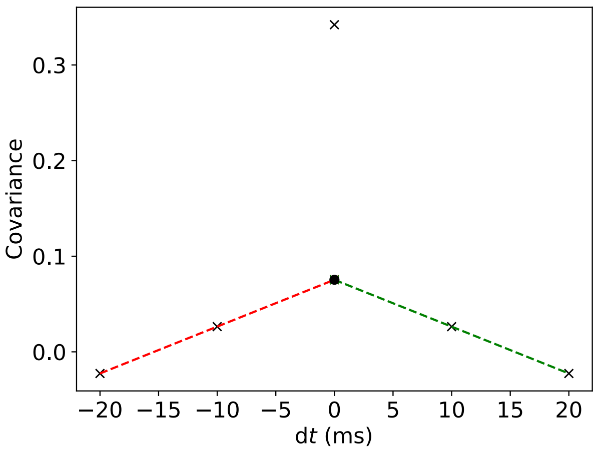

Figure 3. Scintillation co-variance as a function of temporal delay. A linear fit is used to extrapolate to zero temporal delay in order to estimate the scintillation co-variance due to the dome turbulence. The red and green dashed lines indicate the linear fit in the forward and backward temporal direction. The central point at 0.35 is the covariance of all of the turbulence superimposed. This is why we need to examine the spatio-temporal co-variance function and not just the spatial function.

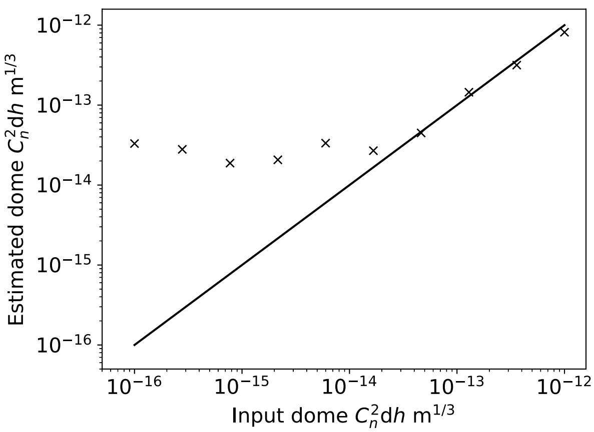

Figure 4. Expected sensitivity to dome turbulence. As expected from simulation, the response is linear to a sensitivity limit of approximately 3×10^{-14} m$^{1/3}$. This limit could be improved (lowered) by conjugating the detector further from the telescope pupil, however, for the purpose of understanding and minimizing local turbulence weak turbulence is less important.

Figure 5. Photo of the DTM bore sighted with the ESA OGS, Tenerife, Spain.

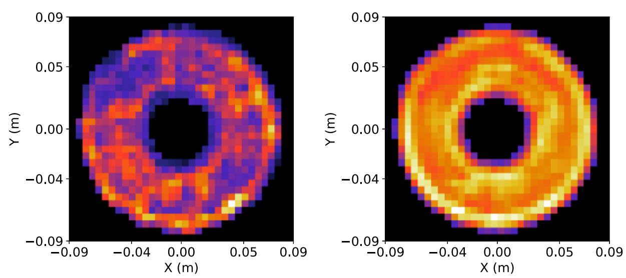

Figure 6. Example conjugated image to +450 m from measured data. Left is instantaneous image and right is average image.

dt = 0. We can then convert scintillation variance, C, to refractive index structure constant, dome, using,

$$C^2_{N,\mathrm{dome}} = \frac{C}{19.2\lambda^{(-7/6)} h_{\mathrm{conj}}^{(5/6)}}, \quad (1)$$

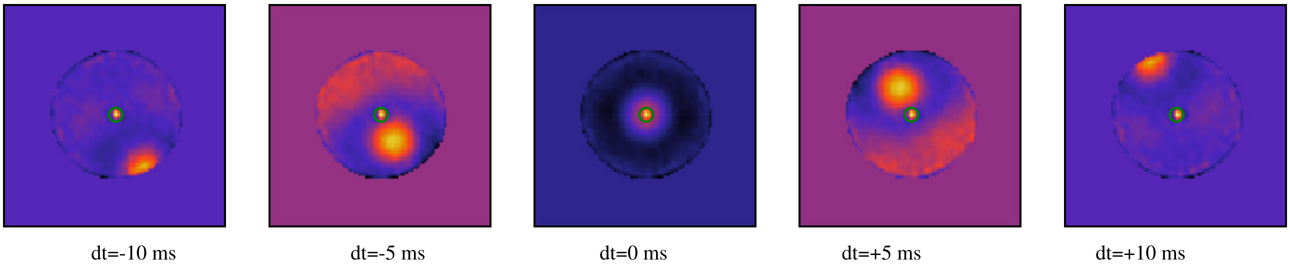

Figure 7. Example spatio-temporal co-variance function measured at the OGS. The central peak is caused by the constrained dome turbuelnce. The larger peak that moves from bottom left to top right is caused by a dominant layer in the free atmosphere. The movement across the function is caused by wind. In this case the frame rate was too high as the free-atmosphere layer is overlaid on the central peak even with dt = +/−5 ms. To mitigate this we use dt = +/−10 ms as our minimum temporal delay. Note that the colour scale changes for each image for clarity.

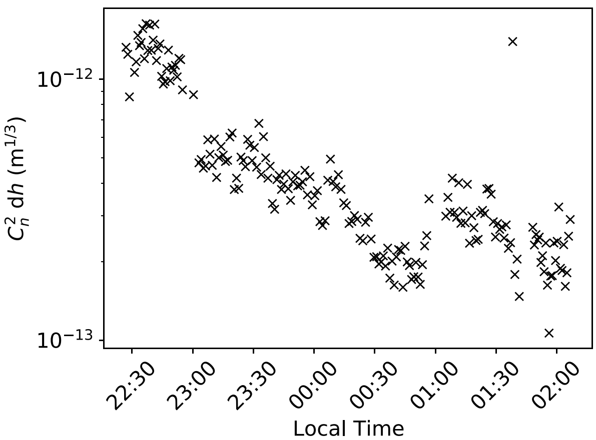

Figure 8. A sequence of the measured dome turbulence at the OGS for the night of 20/09/2022. The data shows very strong turbulence early in the night which drops until approximately local midnight. No effort was made to minimize the dome turbulence during this campaign. There is an obvious outlier at approximately 01:30 which corresponds with the time that people were in the dome.

where, λ is the wavelength of the light and h_{conj} is the altitude that the image is conjugated to.

The advantage of this method is that it is insensitive to shot noise as it is based on the temporal co-variance of frames. The noise is independent in each image and so has little effect on the result. The limitation of sensitivity is due to convergence noise – structure in the 2D covariance function due to correlations between the images than do not average out over the observing period. Fig. 4 shows the simulated response for a range of input dome turbulence magnitudes. The limit of sensitivity is found to be approximately 3×10^{-14} m$^{1/3}$ (corresponding to a coherence length of 0.66 cm, Kolmogorov seeing of 0.31 arcsec at 500 nm). The sensitivity could be improved by conjugating the imager further from the telescope pupil, amplifying the signal from the pupil plane. However, monitoring the dome turbulence is most critical when the turbulence is strong. It is less important to measure weak dome turbulence has it has a minimal effect on the optical image.

The simulation is a full end-to-end Monte Carlo simulation using Fresnel propagation between layers. We build the simulation using the AOTOOLS PYTHON package (Townson et al. 2019). The simulation includes shot noise for a 5th magnitude star in the'V'-band. The simulation runs at a high-spatial resolution and is down sampled to 0.5 cm projected pixel size in order to avoid issues caused by undersampling in the simulation. The dome turbulence is simulated using a slow phase-screen (0.1 m s^{-1}) with an outer scale the of 1 m, boiling is simulated by slowly transferring power between independent phase screens. The simulated time is 1 min of data per measurement.

3 ON-SKY DEMONSTRATION

As a demonstration, we use a small 18 cm f#10 Maksutov telescope attached to the ESA OGS in Izaña, Tenerife (16° 30 arcmin 36.36 arcsec W, 28° 17 arcmin 58.29 arcsec N, 2393 m altitude above sea level). The DTM is boresighted with the OGS, see Fig. 5. The instrument parameters are similar as for the simulation. The frame rate was approximately 400 Hz and we use 1 min data to make a measurement. The exposure time was set to 2 ms. Due to the camera available our projected pixel scale was 1.5 mm. We binned the pixels 10 x 10 to make 1.5 cm super pixels. This speeds up the analysis and matches the simulation work for consistency.

Fig. 6 shows an example of the raw data from the instrument. This can be compared with the simulation data in Fig. 1.

Fig. 7 shows slices of the spatio-temporal co-variance function. Most atmospheric layers are attenuated by the positive conjugate altitude and are not visible. There is a strong high-altitude layer visible and can be seen moving from bottom to top in the images. This layer is moving with the wind-speed of the high-altitude-layer, we know it is a high-altitude layer as the size of the large covariance peak suggests that it is approximately 10 km from the observing plane. The central peak that does not appear to move in the images is due to the turbulence constrained within the dome.

Fig. 8 shows a sequence of dome turbulence strength measured over 4 h at the ESA OGS, Tenerife, Spain, on the night of 2022 September 20th. The sequence shows that the local turbulence was initially very strong and dropped until levelling out to a value of approximately $C_n^2 \mathrm{d}h = 2 \times 10^{-13}$ m$^{1/3}$.

4 CONCLUSIONS

We present a new concept for measuring the local turbulence in an optical telescope dome. The DTM is based on the well known SCIDAR dome monitoring technique, but by extracting only this functionality we show the technique can be performed on a small <20 cm telescope observing a single bright star. Operationally, the DTM could be mounted on the primary mirror cell of a larger telescope and target bright stars through the dome. This arrangement would lead to the DTM measuring the local turbulence along the same line of sight as the main telescope. This is an important capability that has not been previously developed.

Monitoring the dome turbulence is important for several reasons:

(i) active monitoring and minimization of dome turbulence through control of local environment
(ii) optical instrumentation modelling – particularly Adaptive Optics
(iii) PSF reconstruction
(iv) observation scheduling by augmenting external site measurements

This monitor will provide a quantitative measurement of the turbulence in the dome, but not the power spectrum of effective outer scale of the turbulence. This is an advantage and a disadvantage. By exploiting the amplitude of the wavefront rather than the phase, we can make a quantitative measurement of the strength of the turbulence that is insensitive to the nature of the turbulence. However, without knowing the outer scale and power spectrum it is difficult to then convert this into predicted IQ metrics.

Through detailed Monte Carlo simulation, we show that the current design has a sensitivity limit of approximately $C_n^2 \mathrm{d}h = 3 \times 10^{-13}$ m$^{1/3}$ (corresponding to a coherence length of 0.66 cm at 500 nm). This could be improved by using conjugating the detector further from the pupil plane. Although, we believe this to be sufficient for the applications listed above, where measuring strong turbulence is the goal.

An on-sky demonstration was performed at the ESA OGS, Tenerife, Spain. We found that The turbulence in the dome was very strong at the beginning of the night and reduced to a value of approximately $C_n^2 \mathrm{d}h = 2 \times 10^{-13}$ m$^{1/3}$ by mid-night. It should be noted that this was a demonstration of the technique and not a comment on this particular dome. No effort was made to reduce the dome turbulence before or during the test.

ACKNOWLEDGEMENTS

JO is supported by UK Research and Innovation (Future Leaders Fellowship MR/S035338/1).

We would like to thank the European Space Agency (ESA) for access to the Optical Ground Station on Tenerife and the local staff for supporting our work.

This research made use of PYTHON including NUMPY and SCIPY (van der Walt, Colbert & Varoquaux 2011), MATPLOTLIB (Hunter 2007) and ASTROPY, a community-developed core PYTHON package for Astronomy (Robitaille et al. 2013). FAST also makes extensive use of the PYTHON AO utility library AOTOOLS (Townson et al. 2019).

DATA AVAILABILITY

The raw data for the on-sky demonstration is available on reasonable request to the author.

REFERENCES

Avila R., Vernin J., Cuevas S., 1998, Publ. Astron. Soc. Pac., 110, 1106
Beltramo-Martin O. et al., 2020, in Schreiber L., Schmidt D., Vernet E., eds, Proc. SPIE Conf. Ser. Vol. 11448, Adaptive Optics Systems VII. SPIE, Bellingham, p. 114480A
Berdja A., Osborn J., Sarazin M., Dali Ali W., Ziad A., 2013, in Esposito Simone, Fini Lucaeds., Proc. of the third AO4ELT Conf., p. 60
Bustos E., Tokovinin A., 2018, in Marshall H. K., Spyromilio J., eds, Proc. SPIE Conf. Ser. Vol. 10700, Ground-based and Airborne Telescopes VII. SPIE, Bellingham, p. 107000Q
Chabé J., Blary F., Ziad A., Borgnino J., Fanteï-Caujolle Y., Liotard A., Falzon F., 2016, Appl. Opt., 55, 7068
Hunter J. D., 2007, Comput. Sci. Eng., 9, 90
Lai O., Withington J. K., Laugier R., Chun M., 2019, MNRAS, 484, 5568
Racine R., Salmon D., Cowley D., Sokva J., 1991, Publ. Astron. Soc. Pac., 103, 1020
Robitaille T. P. et al., 2013, A&A, 558, A33
Shepherd H. W., Osborn J., Wilson R. W., Butterley T., Avila R., Dhillon V. S., Morris T. J., 2013, MNRAS, 437, 3568
Tokovinin A., 2002, Publ. Astron. Soc. Pac., 114, 1156
Townson M. J., Farley O. J. D., Orban de Xivry G., Osborn J., Reeves A. P., 2019, Opt. Express, 27, 31316
van der Walt S., Colbert S. C., Varoquaux G., 2011, Comput. Sci. Eng., 13, 22
Woolf N., 1979, Publ. Astron. Soc. Pac., 91, 523

This paper has been typeset from a TEX/LATEX file prepared by the author.